

Effect of firing temperature on electrical and structural characteristics of screen printed TiO₂ thick films

C. G. DIGHAVKAR*, A. V. PATIL, R. Y. BORSE^a, S. J. PATIL^a

L.V.H.College, Panchavati, Nashik (Pin 422003), Maharashtra, India.

^aThin and Thick film Laboratory, Dept. of Electronics M.S.G.College, Malegaon Camp (Pin 423105), Dist. Nashik, Maharashtra, India

TiO₂ thick films were prepared by using standard screen printing technique and fired at different temperatures in air atmosphere. The DC resistance of the films was measured by half bridge method in air atmosphere at different temperatures. The films were showing decrease in resistance with increase in temperature indicating semiconductor behaviour. The resistivity, activation energy and temperature coefficient of resistance (TCR) are evaluated at different firing temperatures. The structural behaviour, surface morphology and phase composition were studied by XRD, SEM and EDX technique respectively.

(Received September 02, 2009; accepted October 01, 2009)

Keywords: TiO₂, Thick films, Resistivity, Activation energy, TCR

1. Introduction

Titanium oxide (TiO₂) has been extensively studied owing to its wide range of applications which include photocatalysis, heterogeneous catalysis, energy storage, solar cell components, corrosion-protective coatings and optical coatings [1–5]. Titanium dioxide can be synthesized in three crystalline phases: rutile, brookite and anatase [6]. Titanium dioxide in the anatase crystalline phase is one of the most studied materials for photocatalysis. Among the various metal oxides that can be used in gas sensors, only those materials based on stannic oxide and titanium oxide have been widely manufactured and utilized [7]. The aforementioned background justifies the need to improve the properties and features of these oxides in order to obtain a more efficient material for gas sensing purposes. Several deposition methods have been used to grow undoped and doped TiO₂ films such as Spray pyrolysis, Vacuum evaporation, chemical vapor deposition, magnetron sputtering, pulsed laser deposition, sol-gel technique, screen printing technique [8]. Screen printing technique was introduced in the later part of 1950's to produce compact, robust and relatively inexpensive hybrid circuit for many purposes. Later on thick film technique has attracted by the sensor field [9]. Screen printing is viable and economical method to produce thick films of various materials [10-17]. Thick films are suitable for gas or humidity sensors since the gas sensing properties are related to the material surface and the gases are always adsorbed and react with the films surface [18].

Thick film resistivity can be controlled by the deposition process to sufficiently low value. Its electrical

conductivity is mainly due to Titanium excess at interstitial position. The electrical properties of thick films are functions of several factors [19] such as ingredients, manufacturing technique and sintering history. The ingredients of thick film include a conducting paste of an oxide powder, glass frit and an insulating substrate alumina.

The present work deals with preparation procedure of TiO₂ thick films by screen printing technique and study their electrical and structural properties at different firing temperatures

2. Experimental

2.1 Powder and paste preparation

The TiO₂ powder (AR grade, 99.99%) was weighed and calcined in air at 400°C for 2 hrs. The calcined TiO₂ powder was crushed and mixed thoroughly with glass frit as permanent binder and ethyl cellulose as a temporary binder. The mixture was then mixed with butyl carbitol acetate as a vehicle to make the paste.

2.2 Thick film preparation

Fig. 1 shows the process sequence diagram for preparation of TiO₂ thick films. The paste was used to prepare thick films on alumina substrate by using standard screen printing technique using 140s mesh no. 355. After screen printing, the films were dried under IR-lamp for 60 minutes and then fired at temperatures of 800°C, 900°C, 1000°C for 2 hrs in muffle furnace.

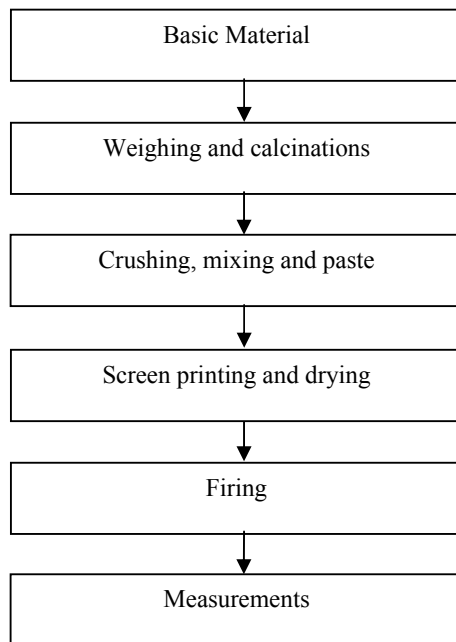


Fig. 1. Process sequence for thick film preparation.

2.3 Thickness measurements

The thickness of the TiO₂ thick films was measured by using Taylor-Hobson (Taly-step UK) system. The thickness of the films was observed uniform in the range of 20 μm to 22 μm (Classic 5175 DM, ±0.5%) across the resistor R_L. Digital temperature controller/monitor system with Chromel-alumel thermocouple was used to indicate the operating temperature. The resistance of the thick film (R_s) was calculated by the relation,

$$R_s = R_L \left(\frac{V_{app}}{V_o} - 1 \right) \quad (1)$$

where V_{app} – Applied voltage, V_o – Voltage across external resistor R_L.

The resistivity value of each film was calculated from the dimensions of the film TCR were evaluated from the observed data in the temperature range 30 - 500 °C.

2.4 Electrical characterization

The DC resistance of the films was measured by using half bridge method as a function of temperature described elsewhere [20, 21]. The films were set in a temperature controlled atmosphere. An external resistor R_L was connected in series with the thick film and fixed DC voltage was applied to the circuit. The values of the film resistance were obtained by measuring output voltage using digital multimeter (classic 5175 DM, ±0.5%) across the resistor R_L. Digital temp

2.5 Structural and morphological Studies

Using X-ray diffraction (Miniflex Model, Rigaku, Japan) analysis from 20-80°, 2θ was carried out to examine the final compositions of the TiO₂ thick films samples. The average grain sizes of titanium dioxide thick film samples were calculated by using the Debye-Scherrer formula [22],

$$D = \frac{0.9\lambda}{\beta \cos \theta} \quad (2)$$

where D is the average grain size, λ = 0.1542 nm (X-ray wavelength), and β is the peak FWHM in radiation and θ is diffraction peak position. The surface morphology and chemical composition of the films were analyzed using a Scanning electron microscope [SEM model JEOL 6300 (LA) Germany] coupled with an energy dispersive spectrometer (EDS JEOL, JED-2300, Germany).

The details of preparation, XRD information and grain size of the films are given in Table 1.

Table 1. Details of the preparation and XRD information of TiO₂ thick films.

I. Material	Titanium dioxide (AR)
II. Substrate material	Alumina
III. Deposition technique	Screen printing method
IV. Type of screen used	140s-mesh no. 355
V. Settling time	10 min.
VI. Drying under IR time	60 min.
VII. Firing time	2 hrs.
VIII. Peak firing temperature	800, 900, 1000 °C
IX. XRD details	Rigaku diffractometer, Miniflex model Japan
X. SEM and EDX detail	JEOL6300 (LA) with JED-2300

3. Results and discussion

3.1 X-Ray diffraction analysis

The XRD patterns of TiO₂ thick films for various temperatures are shown in figure 1. It indicates that (1 0 1) anatase peak located at 25.8 °C for temperatures of 800 & 900 °C. This is the most pronounced peak of an anatase structure. All values of (hkl) are matched by JCPDS data 21-1272 and 21-1276 for anatase and rutile respectively [23]. Up to 900 °C temperatures both the phases of anatase and rutile were found. At 1000 °C firing temperature only rutile phase found. This reduction of intensity indicates a decrease in the anatase content of the TiO₂ film, while the increase in width indicates a decrease in anatase grain size. These are also similar to that has been reported [24]. The anatase peak decreases in intensity at 900 °C temperature and at 1000 °C it disappears. It is clearly shown that phase transformation takes place up to

900 °C and at 1000 °C only rutile phase found. The crystallite size measurements were also carried out using the Scherrer equation [25].

$$D = 0.9\lambda / \beta \cos \theta, \quad (3)$$

where D is the crystallite size, λ , the wavelength of the X-ray radiation (1.54056 Å), β , the line width and θ , the angle of diffraction. The average particle size obtained for anatase and rutile phases from XRD data are 17.86 nm and 37.99 nm respectively.

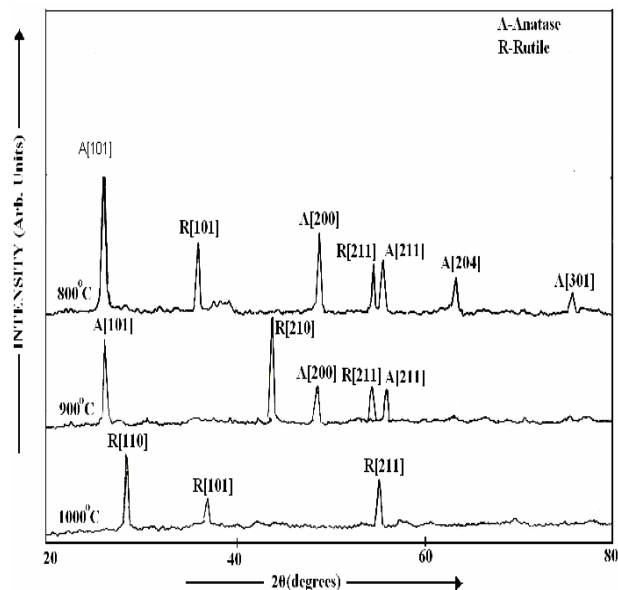
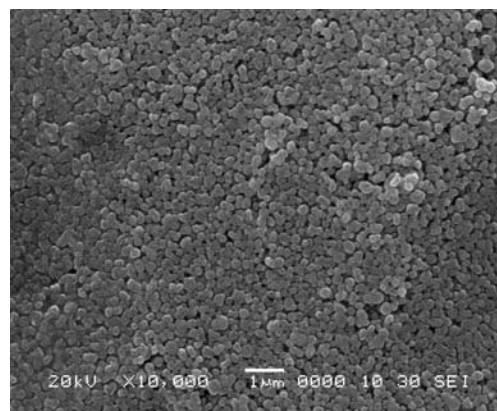


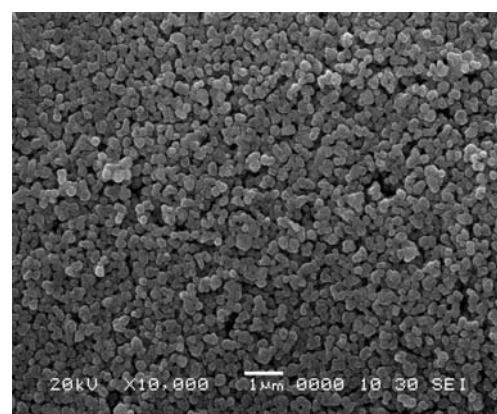
Fig. 2. XRD pattern of TiO₂ Thick films fired at 800 °C, 900 °C, 1000 °C.

3.2 Surface morphology analysis

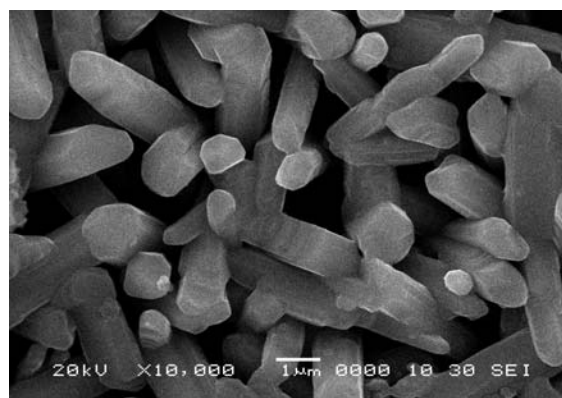
Fig. 3 shows SEM images of TiO₂ thick film fired at 800 °C, 900 °C and 1000 °C. Micro structural characterization was carried out by using scanning electron microscopy. SEM indicated that the microstructure is nearly uniform with negligible open porosity. However presence of some residual, intragranular porosity was seen. It is found that the grain size and the crystalline quality increased with increase in firing temperature. The firing increases the atomic mobility; the atoms can be moved to more energetically favoured sites such as voids, grain boundaries and interstitial positions. An increase in temperature improves the crystallinity and thus increases the mobility of atoms at the surface of films. The film fired at 1000°C resulted in growth of hexadecagonal shaped crystallite of phase oriented at (110) plane which result in uncontrolled growth of grain molecule [26]. The film fired at 800°C exhibits good adhesion. Therefore it can be used for further application work.



(a)



(b)



(c)

Fig. 3. (a) SEM of TiO₂ for firing at 800°C; (b) SEM of TiO₂ for firing at 900°C; (c) SEM of TiO₂ for firing at 1000°C.

3.3 Elemental analysis

It is evident from Table 1. Which is obtained from Energy Dispersive spectrum of TiO₂ for 800, 900 and 1000 °C were compositional measurement have done which shows that by firing excess oxygen is released. [27].

Table 1. Quantitative elemental analysis of TiO₂ films obtained from EDAX.

Firing Temp. Sample- TiO ₂	800 ^o C	900 ^o C	1000 ^o C
Ti (Mass %)	57.63	59.92	60.27
O (Mass %)	42.37	40.08	39.73
Total	100.00	100.00	100.00

From the analysis it was found that TiO₂ films are non-stoichiometry. This behavior is more useful in gas sensing applications.

3.4 Electrical characteristics

Fig. 4 shows variation of resistance with Temperature for TiO₂ thick films fired at temperatures 800, 900, 1000 °C respectively in air. The plot shows different conduction regions: (i) continuous fall of resistance, (ii) an exponential fall region and (iii) finally saturation region. There is decrease in resistance with increase in temperature, indicating semiconducting behaviour. Any increase in temperature of thick film causes the electrons to acquire enough energy and cross the barrier at grain boundaries [28, 29]. There can be decrease in potential barrier at grain boundaries, since at higher temperatures the oxygen adsorbates are desorbed from the surface of the films [28, 30]. Also at higher temperatures the carrier concentration increases due to intrinsic thermal excitation and electron emission process improves with increase in temperature [31]. The thick film shows decrease in resistance with increase in temperature is due to increasing drift mobility of the charge carriers or due to lattice vibrations associated with increasing temperature, where the atoms occasionally come close enough for the transfer of the charge carriers and the conduction is induced by lattice vibration [28].

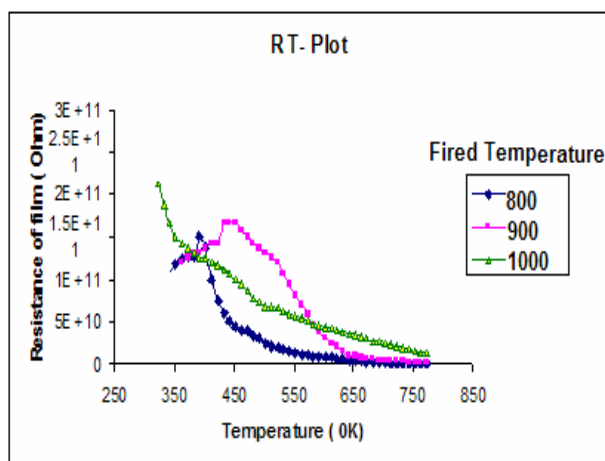


Fig. 4. Variation of resistance with temperature of TiO₂ thick films fired at 800, 900, 1000 °C.

Fig. 5 shows Arrhenius plot of LOG R versus 1/T for TiO₂ thick films. The activation energy in the low

temperature region is always less than the energy in the high temperature region because material passes from one conduction mechanism to another [28, 31]. In the low temperature region, the increase in conductivity is due to the mobility of charge carrier, which is dependent on the defects/dislocation concentration. So the conduction mechanism is usually called the region of low temperature conduction. In this region activation energy decreases because a small thermal energy is quite sufficient for the activation of charge carriers to take part in the conduction process. In other words, the vacancies/defects weakly attached in the lattice can easily migrate. Hence, an increase in conductivity in the lower temperature region can be attributed to the increase of charge mobility.

In the high temperature region, the activation energy is higher than that of the low temperature region. In this region, the electrical conductivity is mainly determined by intrinsic defects and hence is called intrinsic conduction. The high values of activation energy in this region may be attributed to the fact that the energy needed to form the defects is much larger than the energy required for their drift. That is why the intrinsic defects caused by thermal fluctuations determine the electrical conductance of the films only at elevated temperature. [28, 31].

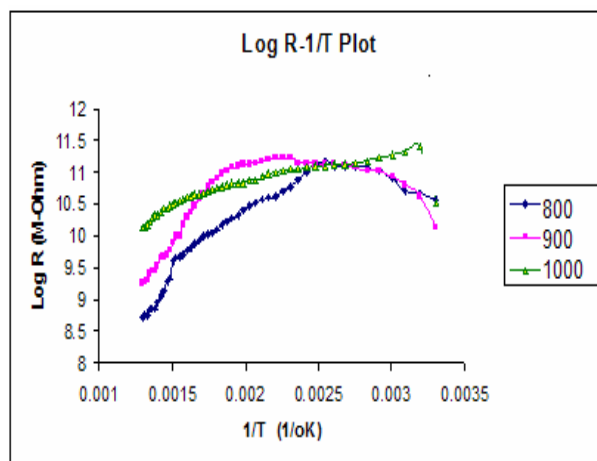


Fig. 5. Plot of LOG R Vs 1/T of TiO₂ thick films fired at 800, 900, 1000 °C.

The variation of grain size, resistivity, and TCR and activation energies of TiO₂ thick films with firing temperature is summarized in Table 3. It is observed that the resistivity, activation energy decreases while TCR and grain size increase with increasing firing temperature.

These results may be attributed to the increase in the degree of crystallinity with the firing temperature.

Table 3. Grain size, resistivity, TCR and activation energy of TiO₂ thick films fired at different temperatures.

Firing Temp °C	Grain Size, nm	TCR, (°C) at const. Temp. 10 ⁻³	Resistivity (Ω cm) 10 ⁴	Activation energy (eV)	
				L.T. : H.T. Region :	Region
800	19.01	1.1560	1.4900	0.4703	2.4800
900	22.31	2.0440	0.4900	0.1224	0.3949
1000	Non-Spherical	9.452	0.2682	0.0104	0.0425

4. Conclusions

TiO₂ thick films deposited on alumina substrate using screen printing technique and fired at different temperatures were showing semiconductor behaviour. The effect of variation in firing temperature (800-1000 °C) on the thick films was evaluated. It is found that the films fired at 800 °C offer low resistivity, low activation energy and high TCR. It shown good adhesiveness XRD and SEM studies have revealed polycrystalline morphology of TiO₂ thick films. It also shows voids between the particles basically due to evaporation of the organic solvent during the firing of the films. The grain size increases with the firing temperature of the films. The film fired at 800 °C would be better for gas sensing application.

References

- [1] G. Colón, M. Maicu, M. C. Hidalgo, J. A. Navio, Appl. Catal. B: Environ. **67**, 41 (2006).
- [2] J. C. Amezcua, L. Lizama, C. Salcedo, I. Puente, J. M. Dominguez, T. Klimova, Catal. Today **107–108**, 578 (2005).
- [3] B. Wawyzyniak, A. Waldemar, B. J. Tryba, Photoenergy **1**, 2006.
- [4] E. Barborini, G. Bongiorno, A. Forleo, L. Francioso, P. Milani, I. N. Kholmanov, P. Piseri, P. Siciliano, A. M. Taurino, S. Vinaty, Sensors Actuators B **111–112**, 22 (2005).
- [5] K. D. Prabir, M. F. de Lucia, Sensors Actuators B **115**, 1 (2006).
- [6] G. A. Tompsett, G. A. Bowmaker, R. P. Cooney, J. B. Metson, K. A. Rodgers, J. M. Seakins, J. Raman Spectrosc. **26**, 57 (1985).
- [7] K. Ihokura, J. Watson, The Stannic Oxide Gas Sensor: Principles and Applications, Boca Raton, FL: CRC Press, 1994.
- [8] B. Joseph, K. G. Gopalchandran, P. K. Manoj, P. Koshy, V. K. Vaidyan, Bull. Mater. Sci. **22**, 921 (1999).
- [9] N. JaydevDayan, S. R. Sainkar, R. N. Karekar, R. C. Aiyer, Thin Solid Films **325**, 254 (1998).
- [10] B. Krishnan, V. N. Nampoori, Bull. Mater. Sci. **28**, 239 (2005).
- [11] X. Q. Liu, S. W. Tao, Y. S. Shen, Sens. Actuators :B chemical **40**, 161 (1997).
- [12] S. G. Ansari, P. Boroojerdian, S. K. Kulkurni, S. R. Sainkar, R. N. Karekar, R. C. Aiyer, J. of Mater. Sci. **7**, 267 (1996).
- [13] M. Prudenziati, B. Morten, Sens. Actuators **B 10**, 65 (1986).
- [14] J. Kiran, R. B. Pant, S. T. Lakshmi Kumar, Sens. Actuators **B 113**, 823 (2006).
- [15] A. T. Nimal, V. Kumar, A. K. Gupta, Indian J. of Pure and Appl. Phys. **42**, 275 (2004).
- [16] L. A. Patil L., P. A. Wani, S. R. Sainkar, A. Mitra, G. J. Pathak, D. P. Amalnerkar, Mater. Chem. Phys. **55**, 79 (1998).
- [17] C. A. Harper, Handbook of Thick film hybrid Microelectronics, McGraw Hill Book Co. New York, 1974.
- [18] K. Ram Kumar, Thick Film Deposition and Processing Short Term Course on Thin and Thick Film Hybrid Microelectronics, Bangalore **P 12.11** (1986).
- [19] K. M. Anisur Rahman, S. Schneider, A. Martin Seitz, J. Am. Ceram Soc. **80**, 1198 (1997).
- [20] G. Srala Devi, S. Manorama, V. J. Rao, J. Electrochem. Soc. **42**, 2754 (1995).
- [21] Duk-Dong Lee, Sens Actuators **B1**, 231 (1990).
- [22] B. D. Cullity, Elements of X-ray diffraction, Addison-Wesley, 102 (1970).
- [23] JCPDS Data 21-1272 and 21-1276.
- [24] G. Mangamma, M. Kamruddin, T. N. Sairam, P. K. Ajikumar, R. Nithya, S. Dash, K. Tyagi, Material Science Div. Indira Gandhi Centre for Atomic Research, Kalpakkam, March 2008.
- [25] B. D. Cullity, Elements of X-ray diffraction, 2nd Edition Addition Wesley, Reading M.A., 1978.
- [26] E. San Andres, M. Toledano M-Luque, A. del Prado, M. A. Navacerrada, I. Martill, G. Gonzalez-Diaz, J. Vac. Sci. Technol. A **23**(6), (Nov/Dec 2005).
- [27] T. B. Ghosh, A. K. Datta, J. of Applied Physics **94**(7), 2003.
- [28] R. Y. Borse, A. S. Garde, Indian J. Phys. **82**(10), 1319 (2008).
- [29] D. Patranobis, Sensors & Transducers, e Book (**PHI**), 2000.
- [30] H. Windichmann, P. Mark. J. Electrochem. Soc. **126**, 627 (1979).
- [31] I. S. Ahmed, I. K. Frag, Battisha, M. M. El-Rafaay, Indian J. Pure Appl. Phys. **43**, 446 (2005).

*Corresponding author: cgdighavkar@gmail.com